SOCIAL REGULATION OF THE A11 DOPAMINERGIC NUCLEUS IN ZEBRAFISH (*Danio rerio*)

By

Faith K Heagy

July 2023

Director of Thesis: Dr. Fadi A. Issa, Ph.D.

Major Department: Biology

ABSTRACT

Aggression is a universal behavioral feature that is present in majority of social animals. In nature, aggression facilities the formation and stabilization of social relationships and allows animals to divide resources according to rank. In zebrafish, aggressive interactions lead to stable dominance formation that consist of dominants and subordinates. Although social-status-dependent differences in behavior must arise due to neural plasticity, mechanisms of how neural circuits are reconfigured to cope with aggression and social stress are poorly described. Here, I describe how the hypothalamic dopaminergic A11 nucleus is morphologically influenced by social status in male zebrafish. The A11 integrates and relays sensory social information to spinal motor circuits to modulate behavior; thus, the A11 is potentially prone to socially induced plasticity. I hypothesized that morphological plasticity of the A11 is differentially regulated in animals of different social ranks. I tested my hypothesis by combining non-invasive behavioral observations and histological approaches. Specifically, I used Tg(*dat:eGFP*) zebrafish, that specifically express eGFP in the dopaminergic system, to investigate how aggressive interactions affect the A11 morphology and axosomatic network connectivity, then correlated morphological plasticity with

changes in motor behavior. I show that A11 cell number and synaptic connectivity are socially regulated. The number of DAT expressing A11 neurons shifts in socially dominant and subordinate animals as social relationships mature, while synaptic connectivity is increased in subordinates. Secondly, I show that these morphological differences are reversable as social environment evolves and correlate with adaptations in motor activity. Results from this project improve our understanding of how social dominance induces morphological plasticity of social decision-making networks and their influence on behavior.

SOCIAL REGULATION OF THE A11 DOPAMINERGIC NUCLEUS IN ZEBRAFISH (*Danio rerio*)

A Thesis

Presented to the Faculty of the Department of Biology

East Carolina University

In Partial Fulfillment of the Requirements for the Degree

Master of Science in Molecular Biology and Biotechnology

by

Faith K. Heagy

July 2023

SOCIAL REGULATION OF THE A11 DOPAMINERGIC NUCLEUS

IN ZEBRAFISH (*Danio rerio*)

by

Faith K Heagy

APPROVED BY:

DIRECTOR OF

THESIS: _____

Fadi Issa, PhD

COMMITTEE MEMBER: _____

Elizabeth Ables, PhD

COMMITTEE MEMBER: _____

Karen Litwa, PhD

COMMITTEE MEMBER: _____

Stefan Clemens, PhD

CHAIR OF THE DEPARTMENT

OF BIOLOGY: _____

David Chalcraft, PhD

DEAN OF THE

GRADUATE SCHOOL: _____

Kathleen Cox, PhD

ACKNOWLEDGEMENTS

I would like to give a special thanks to all my past lab members including Dr. Katie Clements and Thomas Miller for all the dedicated time and work in producing preliminary results that allowed me to take on the A11 Dopaminergic cell project. I also would like to give a special thanks to past lab members, Alexandra Venuto, Miranda Setneska, Skyler Carrell, and Elena Blain for providing me critical feedback, assistance with data analysis, and all the laughs we have shared in the Issa lab. I would like to sincerely thank Dr. Katie Clements again for assisting me in my thesis project, being a wonderful co-mentor, and a great friend.

I sincerely thank my committee members Drs. Elizabeth Ables, Stefan Clemens, and Karen Litwa for all the guidance, support, and professional feedback throughout my master's thesis. A sincere thank you to the department of Biology at East Carolina University, all professor and mentors who critiqued and shaped me as a graduate student. Lastly, I would like to sincerely thank my mentor, Dr. Fadi Issa, for always supporting me, believing in me, and for preparing me to be a successful researcher.

TABLE OF CONTENTS

LIST OF FIGURES

LIST OF ABBREVIATIONS

5-HT	Serotonin
avpl	Arginine vasopressin-like peptide
DA	Dopamine
DAT	Dopamine active transporter
DDC	Dopa Decarboxylase
Drd1b	Dopamine Type 1 receptor
Drd2	Dopamine type 2 receptor
gnrh3	Gonadotropin-releasing hormone
HIT	Histamine
MAO	Monoamine Oxidase
M-cell	Mauthner Command Neuron
PBS	Phosphate buffered saline
PSD-95	Post synaptic density 95
PVOpa	Paraventricular Organ part a
PVOpb	Paraventricular Organ part b
PT	Posterior Tuberculum
slc6a3	Dopamine reuptake transporter
sstr1	somatostatin receptor 1
TH	Tyrosine Hydroxylase
tph1b	tryptophan hydroxylase 1b
VMAT	Vesicular Monoamine Transporter

CHAPTER I

Introduction

Social aggression.

Aggression is a universal behavioral feature that is present in almost all social animals. It is defined as hostile behaviors exhibited towards other animals of the same species to overpower opponents (Lorenz, K 2005). Motivation underlies aggressive behavior and drives competition within and between species. (Lorenz, K 2005; Watanabe and Yamamoto, 2015). Although aggression has many benefits including securing food, shelter, mates, and establishing social hierarchies, it has negative consequences exhibited in elevated social stress among group members. In humans, aggression and violence can lead to a range of psychological disorders due to social stress that impacts nervous system function with long lasting negative effects (Humble and Berk 2003). Social stress leads to psychological problems including depression, anxiety, reduced immunity, and neurophysiological issues (Cunja-Bang et. al, 2017; Takahashi et. al, 2018). A survey of aggressive individuals with high violent offenses followed by neuroimaging of their brain activity after a provocation showed increased reactivity in the amygdala and striatum (Cunja-Bang, et. al, 2017). Genetically, other studies have shown elevated dopaminergic gene expression including dopamine active transporter (*dat1*) and dopamine type 2 receptor (*drd2*) genes that are linked to pathologically violent and aggressive behaviors (Chen et. al, 2005). The *dat1* gene, now more commonly known as *slc6a3*, influences increased reuptake of dopamine in the presynaptic neuron and is associated with increased violence (T.J. Chen et. al, 2007; Schwab-Reese et. al, 2020). Similar mapping of brain regions associated with aggression have been done in model organisms, including zebrafish (T.J. Chen et. Al, 2007). Filby and colleagues (2010) studied brain regions associated with aggression in female and male zebrafish. They identified five

genes being most expressed throughout all brain regions: *gnrh3* (gonadotropin-releasing hormone), *slc6a3* (dopamine reuptake transporter), *sstr1* (somatostatin receptor 1), *tph1b* (tryptophan hydroxylase 1b), and *avpl* (Arginine vasopressin-like peptide). The brain regions with the highest expressed genes correlating with aggression were in the hypothalamus and telencephalon (Filby et. al, 2010). The elevated expression of *slc6a3* and *tph1b* is of particular interest given the regulatory involvement of dopaminergic pathways in social anxiety, depression, motivation, and aggression (Filby, et. al, 2010; Schwab-Reese et. al, 2020). However, even though it is well established that aggressive interactions have profound effects on the psychology and physiology of many social animals (T.J. Chen et. al, 2007; Filby et. al, 2010; Schwab-Reese et. al, 2020), the cellular mechanisms underlying changes in behavioral patterns are still not well understood (Barrios, et. al 2020).

Zebrafish as a model to study social aggression.

Zebrafish (*Danio rerio*) has emerged as a model organism in scientific research since the 1970s. Specifically, zebrafish have been a valuable model in developmental studies due to their transparency during embryonic development facilitating long-term *in vivo* imaging of developing embryos. Zebrafish hatch within 48 hours, develop major organs by 5 days, and are sex determined by 2 months (Veldman and Lin, 2008). Comparable to humans, zebrafish share 70% similarity in proteins and close to 100% in substrate binding regions which makes a great model for drug-binding studies as well as pharmacological studies (Langheinrich, 2003). Importantly, zebrafish are social and shoal in communal settings. When paired together, they engage in agonistic interactions and form stable social dominance relationships making them a good model to study how aggression affects nervous system function (Miller et. al, 2017; Clements et. al, 2018).

Agonistic interactions including biting and circling lead to dominance formation as early as 1 hour after animals are paired (Barrios et. al, 2020; Oliveira et. al, 2011). Agonistic behaviors are initiated by the fish attacking more, whereas the fish succumbing to the attacks is at the bottom of the tank (Miller et. al, 2017). These interactions are driven by hormonal and neural regulation of brain nuclei involved in social regulation (O'Connell and Hofmann, 2012a; O'Connell and Hofmann, 2012b). Specifically, the dopaminergic system is widely known for its neuromodulatory regulation of motivated behavior, aggression, and regulation of spinal cord motor activity (Clemens et. al, 2006; Weitekamp et. al, 2017).

Dopaminergic regulation of social behaviors

Many neurotransmitters and hormones are known to modulate spinal motor networks (Filby et. al, 2010). For example, the serotonin and dopamine systems are widely known to influence the formation of social hierarchies and social dominance (Watanabe and Yamamoto, 2015). Hormones, including corticosteroids and testosterone, have also been extensively studied and are recognized to influence recognition of behavior across various species (Watanabe and Yamamoto, 2015). Specifically, Dopamine (DA) is a monoamine neurotransmitter with a role in learning, movement, motivated behavior, and reward processing via the Mesolimbic pathway, and is known to regulate spinal neural networks (Ikemoto, 1999). DA is synthesized by Tyrosine Hydroxylase (TH) and Dopa Decarboxylase (DDC). From there, DA is imported into synaptic vesicles by vesicular monoamine transporter (VMAT). Dopamine is released into the synaptic cleft and binds to DA receptors (D1-D5), then it is either broken down by monoamine oxidase (MAO) or recycled back into the presynaptic cell by the DAT (Meiser, 2013). Prior work has shown that descending dopaminergic inputs modulate the activity of the startle escape response and swim

circuits in zebrafish (O'Malley et. al, 1996; Filby et. al, 2010**;** Oliveria et. al, 2011; Ryczko et. al, 2013; Miller et. al, 2017; Barrios et. al, 2020).

Zebrafish startle escape response.

The startle escape response in zebrafish is mediated by the Mauthner cells (M-cell), which consist of a pair of giant interneurons located in the hindbrain (Eaton et. al, 1977). The M-cell startle response is an important auditory reflex behavior for zebrafish survival (Eaton et. al, 2001). The M-cell is activated by auditory or vibrational stimulation leading to muscular contraction on the opposite side of the body allowing the animal to escape from the ensuing threat (Figure 1) (Eaton et. al, 1977). Descending direct and indirect dopaminergic and glycinergic inputs modulate the M-cells' excitability (Pereda et. al, 1994; Bátora et. al, 2021). Importantly, the M-cell is known to be modulated through higher brain nuclei receiving visual input, enhance auditory signals, and relay information to the spinal cord to evoke the startle behavior (Mu et. al, 2012; Haehnel-Taguchi et. al, 2018). Given the importance of visual communication during agonistic interactions, this suggests that M-cell excitability and startle escape response is likely prone to plasticity as animals fight for dominance (Clements et. al, 2018).

Prior work in our lab examined whether social dominance influences motor activities of the M-cell startle escape and swim behaviors. Results showed that differences in M-cell mediated startle escape and swim behaviors of paired male zebrafish shift dramatically as social dominance. matures (Miller et. al, 2017). Within 24 hours, dominant animals increase their swimming activity.

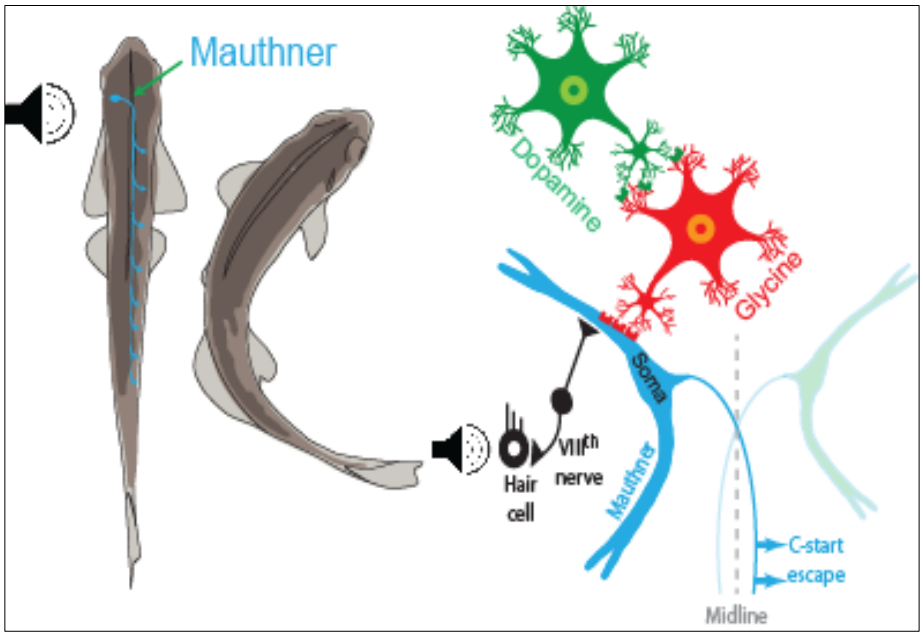

Figure 1. M-cell mediated startle escape circuit in Zebrafish. **A**, M-cell responds auditory stimuli from the VIIIth cranial nerve that innervates the ears. M-cells innervate contralateral motor neurons in the spinal cord. Suprathreshold stimulus induces the escape response (Clements et. al, 2018). M-cell excitability is plastic because of descending modulatory inputs such as dopaminergic (illustrated) and others.

and become less likely to startle, while subordinates display the opposite behavior pattern by reducing their swimming activity and increasing their startle sensitivity (Figure 2A) (Miller et. al, 2017). Although the cellular mechanisms underlying this status-dependent shift in motor activity remain unknown these changes are probably driven by higher brain nuclei, such as the A11 hypothalamic dopaminergic nucleus, that act as integration centers of sensory social information that are relayed to downstream targets to influence motor activity (Mu et. al, 2012; Haehnel-Taguchi et. al, 2018).

Hypothalamic dopaminergic system

The hypothalamus contains numerous dopaminergic nuclei whose function is to regulate behavioral decisions, motivation, aggression, anxiety, and homeostasis (Haehnel-Taguchi et. al, 2018). In previous studies, DA neurons within the posterior tuberculum (PT) located in the hypothalamus, have been examined to send ascending projections to the striatum (Ryczko et al. 2013). DA neurons also send descending projections to the mesencephalic region where dopamine is released affecting locomotion (Ryczko et. al, 2013). The A11 Dopaminergic nucleus is part of the PT. The A11 forms a functional network that receives visual and olfactory information from the optic tectum and olfactory lobe (Mu et. al, 2012), integrates, and relays such information to downstream targets to modulate spinal motor circuits (e.g., startle escape and swim circuits) (Figure 2B) (Haehnel-Taguchi et. al,2018). The A11 neurons also project into the thalamus, other areas of the hypothalamus, dorsal raphe, and the cortex that are also involved in motivated behavior (Koblinger et. al, 2014). The A11 DA neurons consist of two subtypes (type I and type II) with distinct morphological features that facilitate their identification. Type I have large pear-shaped soma with long axonal projections into the spinal cord (Haehnel-Taguchi et. al, 2018). Conversely,

type II A11 cells have small round cells with only local projections (Figure 2B). Other nearby hypothalamic regions surrounding the A11, namely the paraventricular organ part a (PVOpa) and part b (PVOpb), participate in hormonal and homeostatic regulation (Haehnel-Taguchi et. al, 2018). This organization suggests that the A11 type I cells can be a prime target to undergo structural and functional plasticity as animals fight for social dominance. However, the effects of aggression on the morphological and functional organization of the A11 neurons have remain unknown.

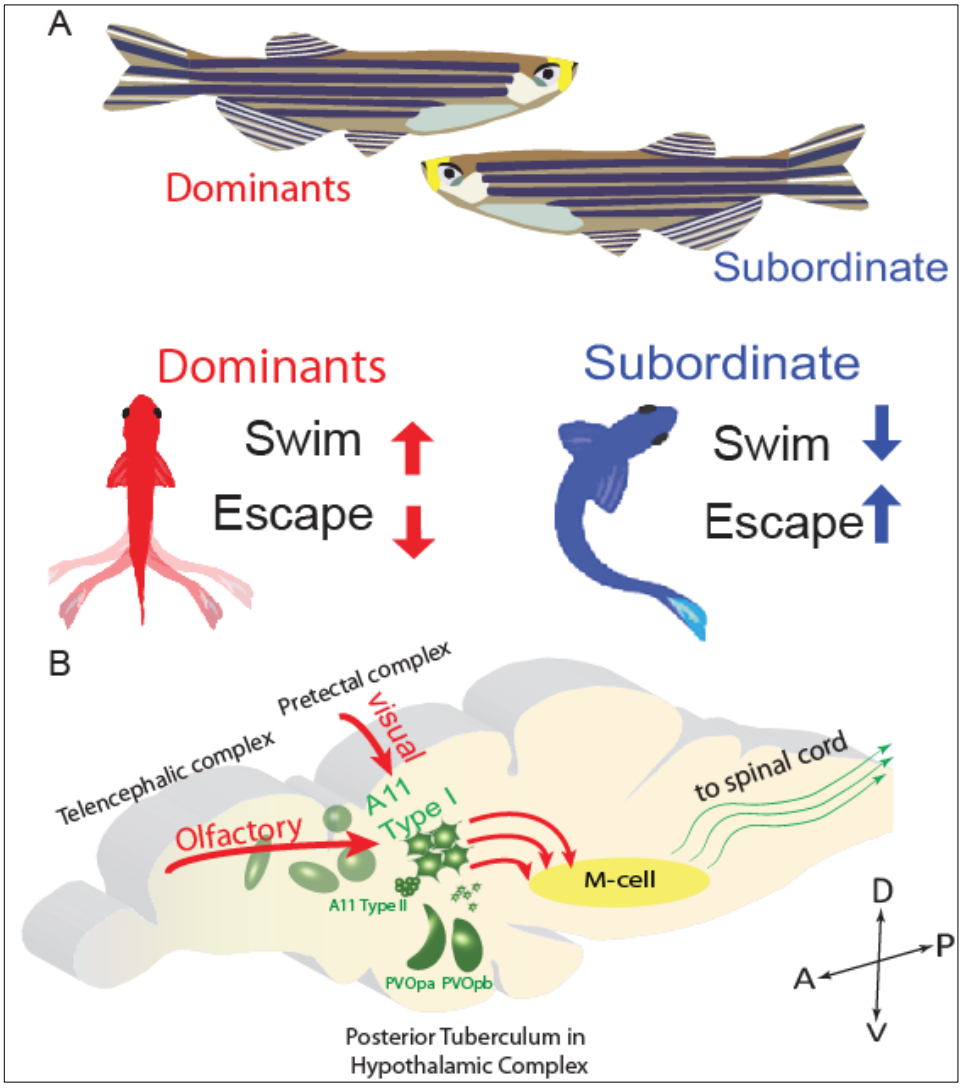

Figure 2: Effect of social status on motor behavior and physiology. **A,** Schematic illustration of the agonistic interactions in male zebrafish and effect of dominance on M-cell mediated startle escape and swim behaviors (Miller et. al 2017). **B,** sagittal view of the zebrafish brain showing dopaminergic nuclei (green ovals) including hypothalamic A11 Type I and type II cells, M-cell (yellow).

CHAPTER 2

Experimental Methods

Animal care and housing.

Zebrafish transgenic line, Tg*(dat:eGFP)* (*Danio rerio*) were maintained in grouped-housed tanks consisting of 15-20 adult zebrafish. The facility was kept at 28 °C under a 10 h dark/14 h light cycle with water pH range of 7.1-7.2. Fish were fed live brine shrimp and pellet food twice daily in the morning and evening. Tg*(dat:eGFP*) line was generated where GFP is expressed under cis-regulatory elements of the *dopamine transporter (dat)* gene (Xi et. al, 2011). The enhanced green fluorescent protein (eGFP) was inserted into *dat* exon 1 by homologous recombination in bacteria (Xi et. al, 2011). Another round of homologous recombination was performed by cloning the 27-kb fragment into a pGEM-Tol2 vector. Following Pre-embryonic injections containing this construct in the presence of the *tol2* transposase mRNA, 90% of embryos expressed eGFP as early as 2 days post fertilization (Xi et. al, 2011). Tg(*dat:eGFP*) F1 generation fish were then crossed with wild-type fish and the progeny was examined (Xi et. al, 2011). Siblings of this generation were kindly given to the Issa Lab by Dr. Tim Erickson (Ph.D, University of New Brunswick). Experiments were conducted according to guidelines approved by East Carolina University's Institutional Animal Care and Use Committee.

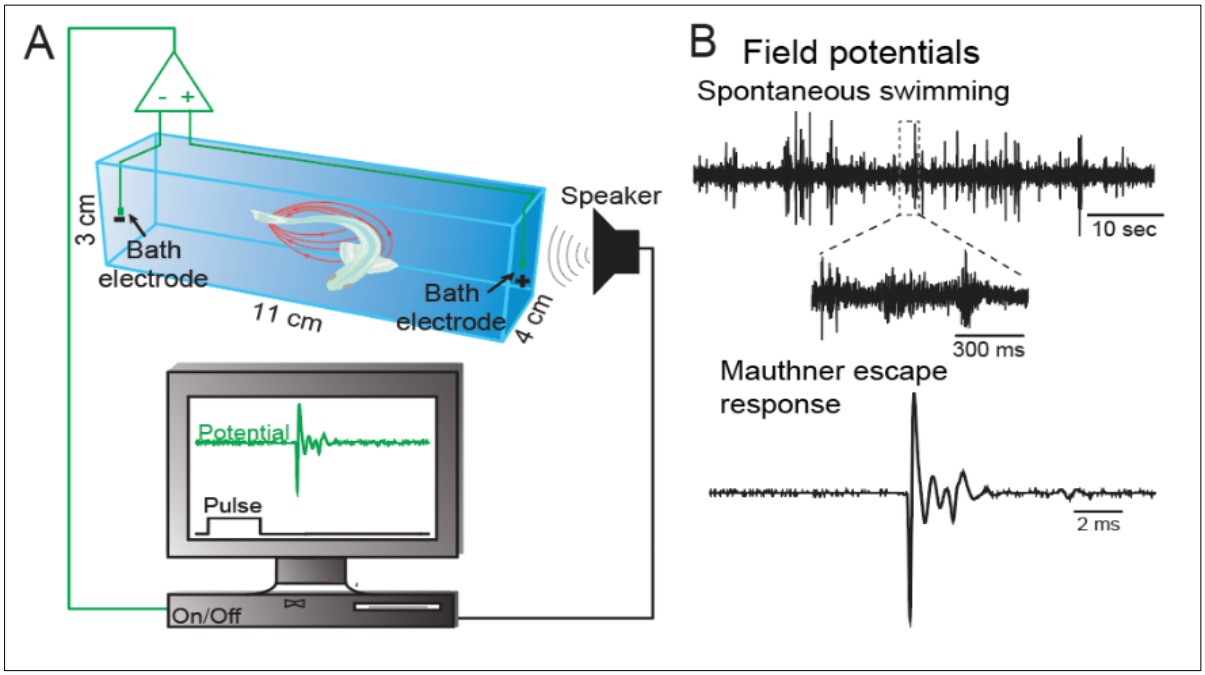

Figure 3. Schematic of experimental setup. A, Bath electrodes detect far-field potentials during swimming and M-cell mediated startle escape behavior in freely behaving zebrafish. **B,** Representative example of spontaneous swimming burst activity (top) and M-cell mediated escape filed potentials (bottom) (Miller et. al, 2017).

Behavioral isolation, pairing, and observation process.

Adult male Tg*(dat:eGFP)* zebrafish, ranging from 3-6 months old, were isolated physically and visually from conspecifics for one week in 23x13x6 cm individual tanks, to minimize prior social experience. Following isolation, two fish of equal size, age, and identical genetic background were paired continuously for seven days, nine days, two weeks, and twenty-eight days. Aggressive interactions were observed daily for 2-3 minutes at mid-day, and the number of attacks and retreats were quantified as described elsewhere (Miller et. al, 2017). Social dominance was determined daily for each pair based on the total number of aggressive attacks (biting and chasing) and defensive retreats. Fish with a high number of attacks were considered dominants while those that retreated from the attacks were considered subordinates.

Behavioral testing.

Using a non-invasive approach, the muscular electric field potentials during M-cell mediated c-start escape and swim behaviors were recorded as described in detail elsewhere (Issa et. al, 2011; Miller et. al, 2017; Clements et. al, 2018). Muscular field potentials were amplified (x1000, AM-Systems, model 1700) and low-pass filtered at 300 Hz and high-pass filtered at 1 KHz before signals were digitized using Digidata 1550 digitizer and stored on a personal computer (Axoscope software, Molecular Devices). Fish were placed individually in a bath electrode chamber and allowed to acclimate for 30 minutes before testing (Figure 3). Following acclimation, one minute of spontaneous swimming activity was recorded. To test escape response sensitivity, auditory pulses at increasing decibels between 0-100 dB were randomly delivered (1 1/2 minutes ISI) at 5dB increments. 1ms square sound pulses were generated using Audacity software. Stimuli

amplitudes were randomized to prevent learning and desensitization effects. Each decibel was repeated 3 times. Data was analyzed using Prism (GraphPad software Inc.) where any large phasic field response within <15 ms of the auditory pulse delivered was considered M-cell mediated escape response. Escape probabilities were determined among all social groups with all values provided as mean and ±SEM.

Reversal behavioral experiments.

Males were isolated for one week then paired together for 14 days. Total numbers of attacks and retreats were tallied, and notes of each animals' physical characteristics were kept for identification. On day 14, two dominants from separate pairs were matched to form a new (Dominant vs. Dominant) pair. Similarly, subordinates from separate pairs were crossed to form a new (Subordinate vs. Subordinate) pair. The new pairs were kept together continuously for an additional 14 days to allow formation of new dominance relationships (Total 28 days of pairing). Behavioral testing of startle sensitivity and swimming activity was carried out as described earlier (Figure 3).

Measuring Swim activity.

Immediately following 30 minutes of acclimation, one-minute of spontaneous swimming activity was recorded for every animal (Axoscope software, Molecular Devices). Swim burst analysis using Clampfit software (Version 11.3, Molecular Devices) was completed by detecting any burst if they are larger than 12 mV in total amplitude and the duration of the burst needed to be in the range of 50-200 ms to be considered a swim burst. At each half-width of burst for all bursts in the one-minute recording, markers were assigned. Any detected signal less than 12 mV was not

marked as it could be considered background noise. Instantaneous frequencies and average number of bursts per one minute were tabulated and graphed in Prism.

Brain tissue extraction, preparation, and slicing.

Extraction of zebrafish brains occurred on days 7, 9, 14, and 28 following behavioral testing of the paired male zebrafish to examine at which time point does the morphology of DAT expressing A11 Type I neurons change as social status-dependent relationships mature. The brains were then placed in a 2 mL microcentrifuge tube containing 1 mL of 4% paraformaldehyde to preserve brain tissue and left over night at 4^{o}C. The following day, brains were washed 4-5 times for 25 minutes in PBS. After washes, brain tissues were moved to another 2 mL microcentrifuge tube and 1 mL of 30% sucrose was added as a cryoprotectant to protect the brain during freezing by minimizing freezing damage. The samples were left overnight in 4^{o}C fridge. The next day, brains were placed in a mold filled with OCT and oriented for sagittal sectioning and flash frozen in liquid nitrogen. Parafilm was wrapped around the molds for storage. If not sliced right away, the tissue was placed in -20° C freezer. OCT embedded brain tissues were placed in a cryostat (Microm HM 550) at -19°C and trim at 100 µm. Once parameters are set, tissue molds were added on a metal chuck and locked into position. Brain tissues were sliced at 30 µm, and 4-5 slices are added onto a Superfrost Plus Microscope slide (Fisher Scientific). Total number of slides per brain averaged around 8-10 with 4-5 slices per slide.

PSD-95 immunostaining.

Post synaptic density-95 (PSD-95) marker was used as a synaptic marker (Abcam) (Han et. al, 2022). Brain slices were washed 3-4 times for 5 minutes each in PBS then placed in 5% bovine

serum and 2% goat serum blocking buffer for 1-2 hours following cryo-sectioning. Another series of PBS washes (3-4 times for 5 minutes) were performed, and slices were stained with a rabbit polyclonal anti-PSD-95 primary antibody (Abcam #Ab19258) at a concentration of 1:200. All slides are appropriately placed overnight in the fridge at 4ºC. Following primary antibody incubation, additional 3-4 PBS washes were performed, and slices incubated for 1-2 hours at room temperature in goat anti-rabbit Alexa Fluor-555 secondary antibodies (Invitrogen #A21428) diluted at a 1:500 concentration. Secondary antibodies were washed in PBS then slides were mounted with one drop of Antifade gold reagent protectant (Invitrogen #P36980). Slides were cured in the fridge for 24 hours then sealed with clear nail polish to protect the tissue from decaying.

Data acquisition and analysis.

Confocal images were obtained using a Carl Zeiss LSM 800 confocal microscope. The lasers 488 and 555 were used to image the A11, PVOpa, and PVOpb regions in all brain slices using 40x oil objective lens. To standardize acquisition across animal groups, acquisition mode settings for the 488 and 555 channel were set as follows: Master gain at 600, laser pinhole at approximately 0.70, and Digital gain range from 3 to -3, with 1µm optical steps, and images were averaged twice. Once imaging was completed, confocal stacks were analyzed using Imaris software (Oxford Instruments, ver. 9.3) for automated cell count and colocalization analysis of the *dat:eGFP* channel to the Alexa fluor-555 channel. Cell count of A11, PVOpa, and PVOpb neurons was conducted by selecting spots function, setting the parameters for region of interest, and using auto count function. Some cells were manually counted when errors were identified. The total number of DAT expressing A11 Type I cells per brain as well as total DAT expressing A11 Type I cells also

expressing PSD-95 were tabulated in Excel, and a ratio for each brain was computed. The average ratio and standard deviations of each social group (communals, dominants, and subordinates) was calculated. Volumetric analysis of A11 cell size was also conducted using Imaris utilizing digital rendering cell surface function.

Statistical Analysis.

Prism (GraphPad, ver.3) was used to generate all graphs and conduct statistical tests. Statistical analysis was performed using One-Way ANOVA test with Kruskal-Wallis multiple comparison post-test, two-tailed. To compare M-cell startle escape response probability among the social groups, the data was curve fitted with a Boltzmann Sigmoidal curve fit with a non-linear regression. One-Way ANOVA tests were performed to compare average number of swim bursts per minute, and the number of DAT expressing A11 Type I neurons at day 7, 9, and 14 of social pairing for each phenotype. A paired t-test was performed on soma volumetric differences between DAT expressing A11 Type I cells and DAT expressing A11 Type II cells as well as comparing DAT expressing A11 Type I cell number between the zebrafish in each dominant reversal pairs and subordinate reversal pairs. Chi-square analysis was performed on PSD-95 expression differences among social phenotype's A11 DAT nucleus. Statistical significance level was set to $p<0.05$.

CHAPTER III

Results

Sensitivity of the M-cell mediated startle response is socially regulated.

Prior work has shown that after 14 days of interactions, patterns of motor activity shifts accordingly to social rank whereby dominants increase their swimming activity and reduce their startle sensitivity, while subordinates reduce their swimming and increase their startle sensitivity (Figure 2A) (Miller et. al, 2017). However, the time course at which these behavioral differences emerge and their relation to changes in brain morphology have not been examined. First, I measured the animals' startle escape sensitivity and swim behavior in dominants and subordinates at 7, 9 and 14 days of social interactions (Figure 4). I hypothesized that during the early periods of dominance formation (days 7 and 9) there will be no social status-dependent differences since social relationships are still solidifying. I found that the sensitivity of startle escape among all groups on day 7 and day 9 showed no significant differences (Figure 4A and B; day 7:communals n=6, dominants n=9, subordinates n=9; day 9: communals n=6, dominants n=6, subordinates n=6) although, there was a diverging trend in startle behavioral response where subordinates were slightly more sensitive and dominants are not responsive as frequently. Those differences between dom vs. sub became progressively more obvious and statistically different by day 14 (Figure 4C; One-Way ANOVA, Kruskal-Wallis post-test, com vs. sub [85dB] $p=0.0434$, [87dB] com vs. dom $p=0.053$, dom vs. sub [90dB] $p=0.0226$, communals n=6, dominants n=6, subordinates n=6).

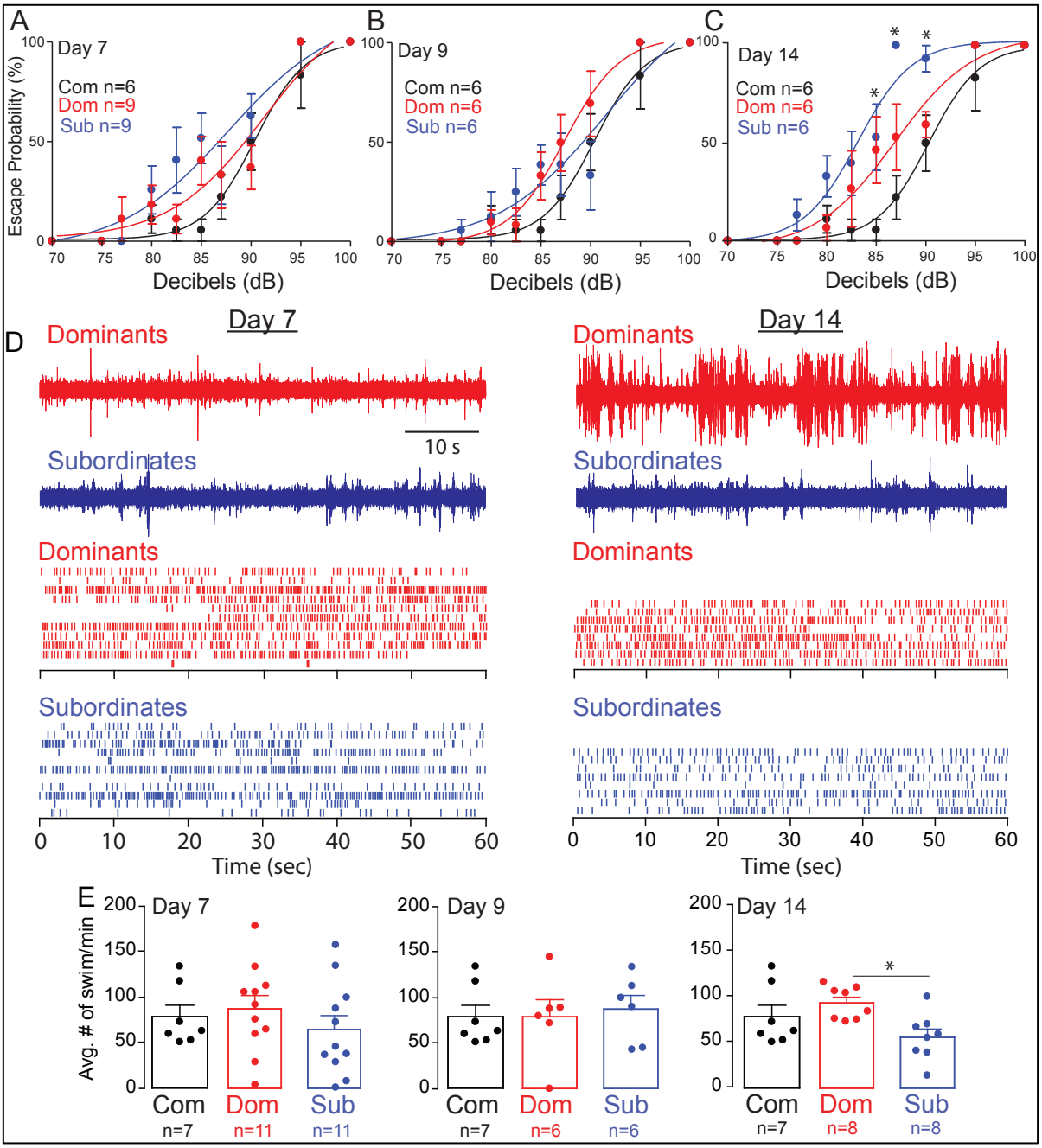

Figure 4: Effect of social status on startle escape response and swim behaviors. **A-C,** startle response probabilities of communals, dominants, and subordinates, on days 7, 9, and 14 of social pairing. **D**, raster plots of swim bursts activity in dominants and subordinates on days 7 and 14 of pairing (communal control data and day 9 is not illustrated, refer to panel E for communal and day 9 data). Each row represents the activity of individual fish, and each circle represents one swim burst. **E**, summary graphs of the average swim bursts per minute among all three social groups. Dots represent average individual fish spontaneous swim activity during a 1-min recording.

Swim behavior is socially regulated. To confirm that social status does affect swim activity, spontaneous swim activity of each individual fish was recorded for one-minute. Knowing from previous results that wild-type dominants swim significantly more by day 14 of pairing compared to subordinates (Miller et. al, 2017), whether behavioral differences exist earlier by days 7 and 9 of pairing was determined. I hypothesized that on days 7 and 9, there would be no differences among all phenotypes. Raster plots were tabulated to show each fish (row) and their associated swim burst within the one-minute recording (Figure 4D). Dominants and subordinates did not vary in spontaneous swim activity on days 7 and 9, but their swimming activity diverged significantly by day 14 of pairing (Figure 4D).

To confirm this observation, the average number of swim bursts per minute among all groups (Figure 4E) was calculated. On day 7 of pairing, there were no differences in swim activity among all social phenotypes (One-Way ANOVA; Kruskal-Wallis post-test, p=0.440; communals n= 7, dominants n= 11, subordinate n= 11). On day 9 of pairing, similar trend occurred as on day 7 where there were no differences in swim activity among all social phenotypes (One-Way ANOVA; Kruskal-Wallis post-test, p=0.8461; communals n=7, dominants n=6, subordinate n=6). However, by day 14 of pairing, dominants swam significantly more compared to subordinates. (One-Way ANOVA, Kruskal-Wallis post-test, p=0.0142; communals n= 7, dominants n= 8, subordinate n= 8).

Social status affects DAT expression in A11 Dopaminergic neurons.

A11 dopaminergic nucleus integrates sensory social information and relay it to spinal cord circuits including the M-cell startle escape circuit. Given the observed differences in escape sensitivity between dominants and subordinates, I hypothesized that the A11 is prone to socially mediated

plasticity. To determine the morphological effects of social status on A11 cells, the A11 nucleus was imaged and the total number of DAT expressing A11 Type I cells in socially dominant, subordinate, and communal controls was quantified (Figure 5A). As noted earlier, A11 nucleus consists of two types of DAT expressing cells, and only type I projects and innervates M-cell circuit. Thus, to ensure accurate identification of type I cells, analysis and comparison of Type I and Type II volumetric soma size (μm^3) was quantified (Figure 5B). They are easily distinguishable due to significant differences in soma volume whereby type I somas were larger in volume compared to type II somas (Figure 5B, t-test, P<0.0001, communal A11 type I: n= 27, A11 Type II n=28). Further, there were no differences in type I cell volume among all three social phenotypes nor was there a correlation in soma volume between dominant and subordinate pairs (Figure 5C, One-Way ANOVA, Kruskal-Wallis post-test, p=0.5008; communal n=9, dominants n=9, subordinates n=9). Next, the number of DAT expressing A11 type I cells on day 7 of social pairing among the three social phenotypes were compared. Communals had significantly higher number of cells compared to dominants and subordinates, but there were no differences between dominants and subordinates (Figure 5D, One-Way ANOVA, Kruskal-Wallis post-test, p=0.0027; communal n=10, dominants n=7, subordinates n=7). By day 9 of social interactions, differences in the number of cells between communals and dominants became insignificant, but those of subordinates remained lower compared to communals only (Figure 5D, One-Way ANOVA, Kruskal-Wallis post-test, p=0.0091; Communal n=10, Dominants n=6, subordinates n=6). However, by day 14, the number of cells between dominants and subordinates became statistically significant (Figure 5D; One-Way ANOVA, Kruskal-Wallis post-test, p=0.0013; communals n=10, dominants n=9, subordinates n=9). Interestingly, the average number of DAT expressing A11 Type I cells on day 7 in dominants and subordinates was similar to those of social isolates (7 days

of isolation without pairing) (Figure 5E). In dominant animals, the average number of DAT expressing A11 Type I neurons gradually increased over time and became significantly higher by day 14 compared to day 7, but the number of cells in subordinates remained consistently lower and comparable to those of social isolates (Figure 5E; One-Way ANOVA, Kruskal-Wallis post-test, $p= 0.0077$, isolates n= 6, dominants day 7 n=7; day 9 n=6, day 14 n=9). These results suggest that the A11 nucleus is prone to social plasticity, in that the number of DAT expressing A11 Type I cells are plastic. Social isolation may induce a modest, albeit insignificant, decline in the number of A11 cells due to stress (One-Way ANOVA, Com vs. Iso. $p>0.05$), but dominants quickly recover while subordinates do not because of continued stress mediated by social subordination.

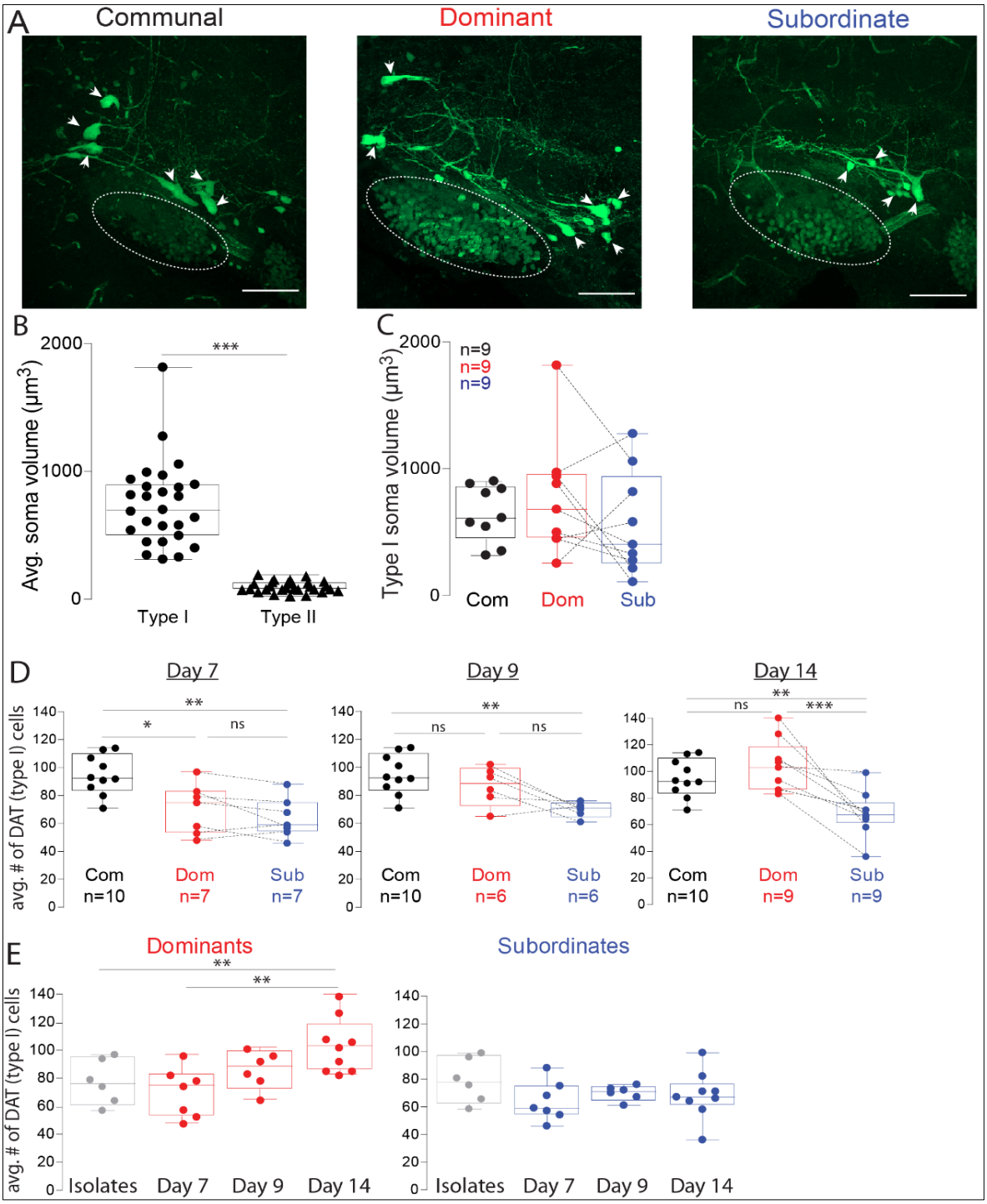

Figure 5: Effect of social status on A11 cell morphology. **A,** representative confocal projections (30 µm thickness) of the A11 nucleus of a communal, dominant, and subordinate animal highlighting the type I (arrowheads) and type II DAT expressing cells (ovals)(scale = 30µm). **B**, average soma volumes for type I and II cells in communal animals. **C**, Box plot comparison of type I soma volume across social groups. Dashed lines denote paired-wise comparison of each dominant to its subordinate counterpart. Box denotes 95% of data, horizontal line within the box denotes median, error bars denote minimum and maximum values. **D**, average number of DAT expressing type I cells on days 7, 9 and 14. **E**, same data as shown in panel D but separately comparing time course changes in the average number of cells for dominants and subordinates relative to social isolates.

Socially mediated plasticity of hypothalamic dopaminergic nuclei is specific.

To determine if the effects of social dominance on dopaminergic nuclei is specific to the A11 or whether the effects extend to other hypothalamic dopaminergic nuclei, I examined the PVOpa and PVOpb nuclei that are adjacent to the A11. The PVOpa and PVOpb axonal projections are local and are thought to be involved in hormonal regulation and homeostasis within the hypothalamus; thus, are unlikely to play a direct role in modulating spinal circuits (Haehnel-Taguchi et. al, 2018). To test this hypothesis, I quantified the number of DAT expressing cells in the PVOpa and PVOpb nuclei in all three social phenotypes (Figure 6A, B). I found no statistical differences among all social groups within the PVOpb (One-Way ANOVA, p=0.4572; Communals n=10, Dominants n=7, Subordinates n=7) and PVOpa regions (Figure 6C and D, One-Way ANOVA, p=0.9407; communals n=10, dominants n=7, subordinates n=7). This result suggests that the effect of social domiannce on brain function is likely limited only to specific dopaminergic nuclei that are involved in social regulation.

Differences in motor activity and plasticity of A11 number are not innate.

The gradual increase or decrease in DAT expression in dominants during the two weeks of social interactions suggested that social factors rather than innate differences underly the observed neural increase (Figure 5E). To investigate the robustness of social influence on A11 cell number, I assessed whether reversal in social conditions would correlate with adaptations in motor behavior and A11 cell number. I hypothesized that the effects of social status on motor behaviors and A11 cell number are socially induced. To test this hypothesis, I paired dominants together to form

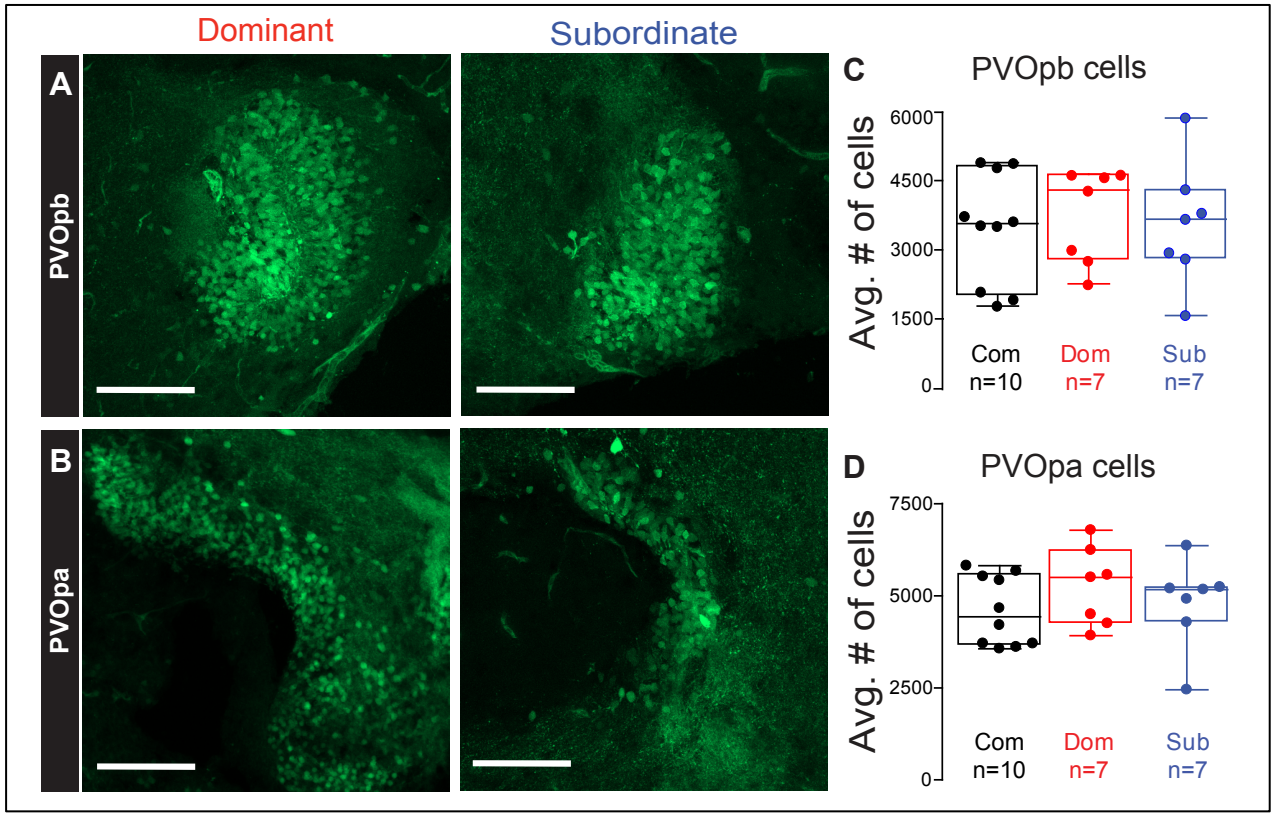

Figure 6: Effect of social status on the PVOpa and PVOpb cell morphology. **A-B**, representative confocal projections of PVOpb and PVOpa hypothalamic nuclei from a dominant and subordinate fish. **C-D**, average number of DAT expressing cells in PVOpb and PVOpa, respectively, among all three social groups.

(dom vs. dom pairs) and subordinates together to form (sub vs. sub pairs) and allowed the new pairs to reestablish new social relationships for an additional 14 days of interactions (Figure 7A). Under this scenario, dom vs. dom pairs, one of the animals would remain dominant while its counterpart would become a subordinate. Conversely, in the sub vs. sub pairs, one of the animals would become dominant while its counterpart would remain a subordinate. During social interactions, the number of attacks and retreats were quantified every day, and identity of each individual fish was tracked by descriptive notes of physical features. After two weeks of social interactions, I measured the animals' startle escape sensitivity, swimming activity, and number of DAT expressing A11 type I cells (Figure 7 B, C, D). In the dominant repairing, the sensitivity of the startle response of the new subordinates (D→S) did not shift significantly compared to their dominant counterparts (D→D) (Figure 7B). However, sensitivity of the startle response differed significantly between new dominants and subordinates in the sub/sub pairs. The sensitivity of the startle response of the new dominants (S→D) declined significantly compared to their subordinate counterparts (S→S) (Figure 7B; two-tailed paired t-test [85dB] $p=0.0313$, $t=4.382$ $df=6$; [87dB] $p=0.0049$, $t=4.336$ $df=6$; $n=7$ pairs). Interestingly, dominant repairs (5 pairs) had a higher death rate compared to the subordinate pairs, therefore further behavioral and morphological experiments could not be conducted. This is due to heightened aggressive attacks between the two dominants, leading to death.

Next, I measured spontaneous swimming activity. In the dominants repairing, swimming frequency of the dominant fish that lost their rank and became subordinates (D→S) declined compared to their dominant counterparts (D→D), however the decline was not statistically significant (Figure 7C, two-tailed paired t-test $p=0.1910$; $t=1.512$ $df=5$, $n=6$ pairs). However, in the subordinate repairing, swimming frequency of the former subordinates that became dominants

(S→D) increased significantly compared to their subordinate counterparts (S→S) (Figure 7C; two-tailed paired t-test p=0.0192; t=3.403 df=5, n=6 pairs). Interestingly, the increase in swimming frequency among the new dominants (S→D) in the subordinate repairing rose nearly to the levels of those of dominants in the dominant repairing (D→D). Finally, comparison in the swimming frequency between dominants in the (dom vs. dom) pairs to the subordinates in the (sub vs. sub) repairs showed significant differences (Figure 7C; two-tailed unpaired t-test p=0.003; t=3.886 df=10, n=6 animals), but there were no significant differences between the subordinates in the (dom vs. dom) pairs compared to the subordinates in the (sub vs. sub) pairs (Figure 7C; two-tailed unpaired t-test p=0.3665, t=0.9459 df=10, n=6 animals).

Finally, I examined the effect of social reversal on the number of DAT expressing A11 cells. In the dominants repairing, the number of A11 type 1 cells in new subordinates (D→S) declined significantly compared to their dominant counterparts (D→D) (Figure 7E, two-tailed paired t-test, p=0.0079; dominants n=6, subordinates n= 5). In the subordinates repairing, I found that the number of A11 type I cells in new dominants (S→D) increased significantly compared to their subordinate counterparts (S→S) (Figure 7E, two-tailed paired t-test, p=0.0057; dominants n=6, subordinates n= 6). Overall, our results suggest that plasticity in DAT expressing A11 cell number is socially regulated.

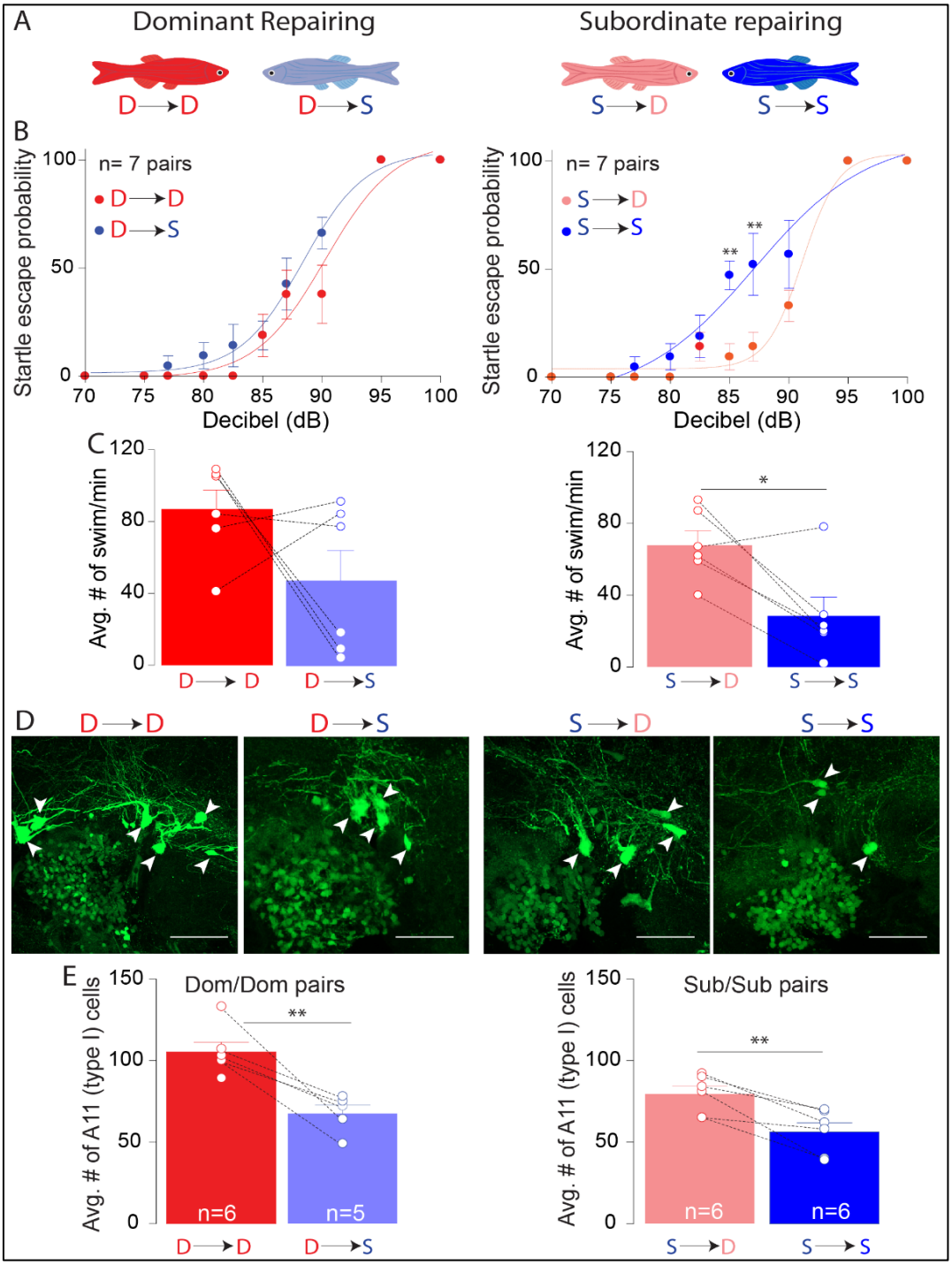

Figure 7: Effect of social reversal on startle sensitivity, swim activity, and A11 cell number. **A**, Schematic illustration of experimental crossings (refer to methods for details). **D**: dominant, **S**: subordinate. **B**, startle escape probability in dominant vs. dominant pairs (left), subordinate vs. subordinate pairs (right). **C**, Average number of swim bursts per minute in dominant pairs (left) and subordinate pairs (right). **D,** representative confocal projections of dominants and subordinates from the (Dom vs Dom) pairs and (Sub vs Sub) pairs. Arrowheads: type I A11 cells (Scale = 30 µm). **E**, average number of A11 cells from the respective animal crossings. Dashed lines denote paired-wise comparison of each dominant to its subordinate counterpart.

Social status affects synaptic plasticity of the A11 cells.

The A11 nucleus forms a functional network with extensive synaptic connectivity among its neurons. Cellular gain or loss is likely to impact its structural and functional organization. However, homeostatic mechanisms may play a significant role ensuring continued network functionality. I hypothesized that the observed differences in A11 cell numbers may lead to compensatory axosomatic connectivity to maintain A11 functional integrity. To test this hypothesis, I stained the A11 nucleus with PSD-95 synaptic marker in socially dominant, subordinate, and communal controls (Figure 8). A ratio for each animal was computed by taking the total number of DAT expressing A11 Type I cells also expressing PSD-95 by the total number of DAT expressing A11 Type I cells. Using the average ratios of each social group, a Chi-square analysis was performed comparing all social phenotypes. On average, 21% (SD=0.061, n=6) of DAT expressing A11 neurons expressed PSD-95 in dominant brains, which is significantly lower from expression in subordinate brains where on average 46% (SD=0.0542, n=6) DAT expressing A11 neurons expressed PSD-95 (Chi-square statistic:14.0276, p=0.0002) (Figure 8B). Communals average DAT A11 PSD-95 expression was 27% (SD=0.0957, n=7) and was not statistically different from dominants (Chi-square statistic: 0.9868, p=0.3205) (Figure 8B). When comparing subordinates average DAT A11 PSD-95 expression to communals' average, there was a statistical difference in PSD-95 expression (Chi-Square statistic 7.7877, p=0.0053). Overall, the results suggest that subordinates have more A11 cells that express PSD-95 compared to communals and dominants.

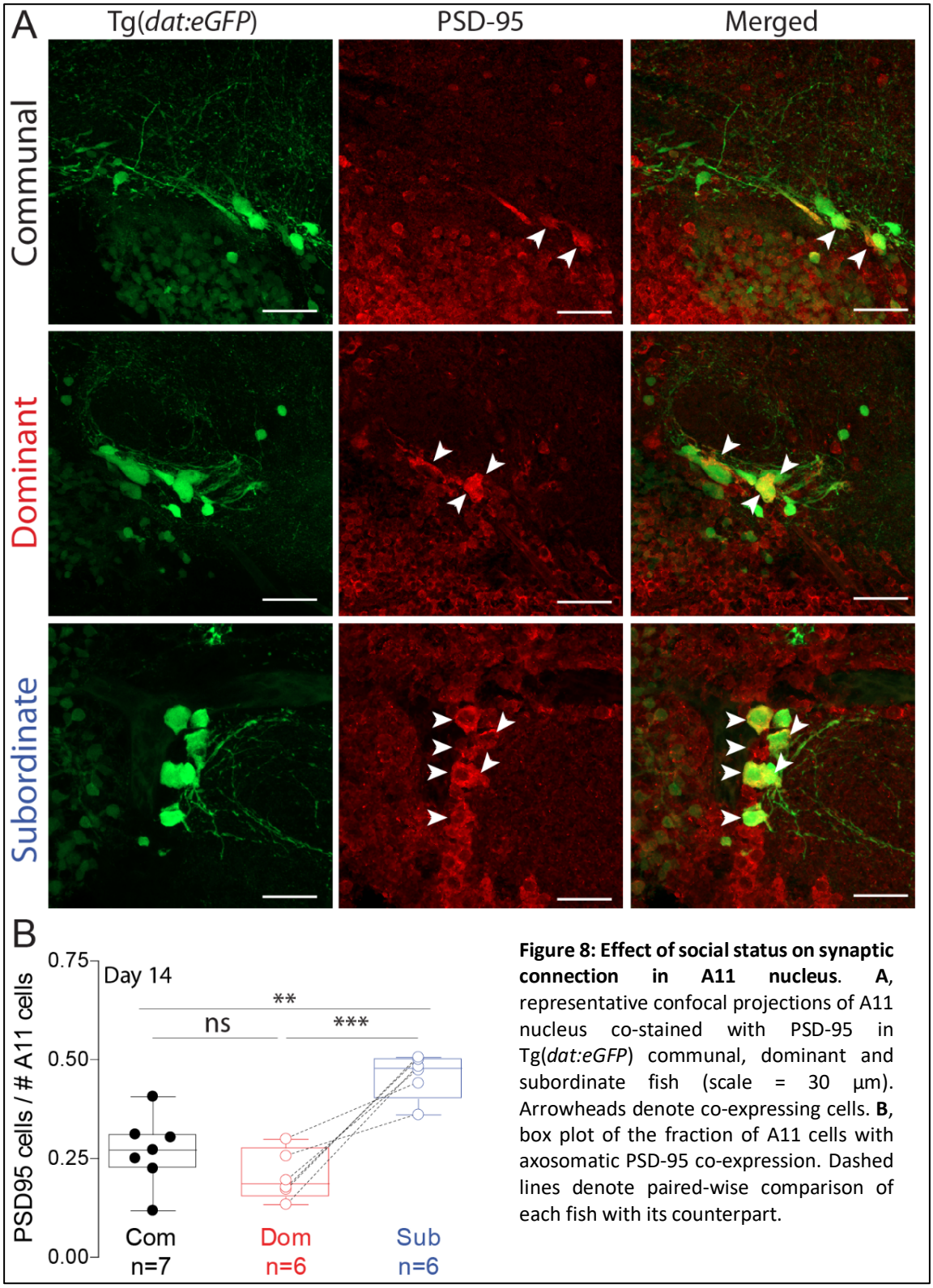

Figure 8: Effect of social status on synaptic connection in A11 nucleus. **A**, representative confocal projections of A11 nucleus co-stained with PSD-95 in Tg(*dat:eGFP*) communal, dominant and subordinate fish (scale = 30 µm). Arrowheads denote co-expressing cells. **B**, box plot of the fraction of A11 cells with axosomatic PSD-95 co-expression. Dashed lines denote paired-wise comparison of each fish with its counterpart.

CHAPTER IV
DISCUSSION

The hypothalamic dopaminergic A11 nucleus integrates and relays social information to the spinal cord to modulate motor activity. Here, I examined the effects of social status on the startle escape and swim behaviors and how behavioral adaptations correlate with morphological plasticity of the A11 nucleus. Three principal conclusions can be drawn from this study. First, as social dominance relationships solidify, the behavior patterns of zebrafish diverge according to social status. Dominant animals increase their swimming activity and reduce their sensitivity of startle escape, while subordinate animals reduce their swimming behavior and increase their startle sensitivity. Secondly, these status-dependent differences correlate with morphological differences in DAT expressing A11 cell number and synaptic interconnectivity. Time course experiments suggest that social dominance promotes proliferation in A11 cell number, and those differences emerge after 9 days of social interactions; while social isolation and subordination induced stress may lead to neuronal loss. Thirdly, socially driven plasticity of DAT expressing A11 cell number is reversable suggesting plasticity in motor behaviors and brain function.

Prior work in our lab suggests possible functional consequences of status-dependent differences in cell number on motor activity. Previously, we have shown that DA signaling indirectly modulates M-cell excitability by regulating glycinergic inputs to inhibit M-cell excitability (Figure 9). Thus, activation of the intermediate glycinergic inhibitory input leads to an inhibition of startle sensitivity (Clements et. al, 2020). It was shown that in dominant animals, increased dopaminergic signaling coupled with increased dopamine receptor type 1 (Drd1) expression in glycinergic neurons strengthens dopaminergic to glycinergic synaptic activity to reduce M-cell excitability (Figure 9). My results support this model by showing an increase in DA cell number, which would in turn increase the synaptic drive between dopaminergic and

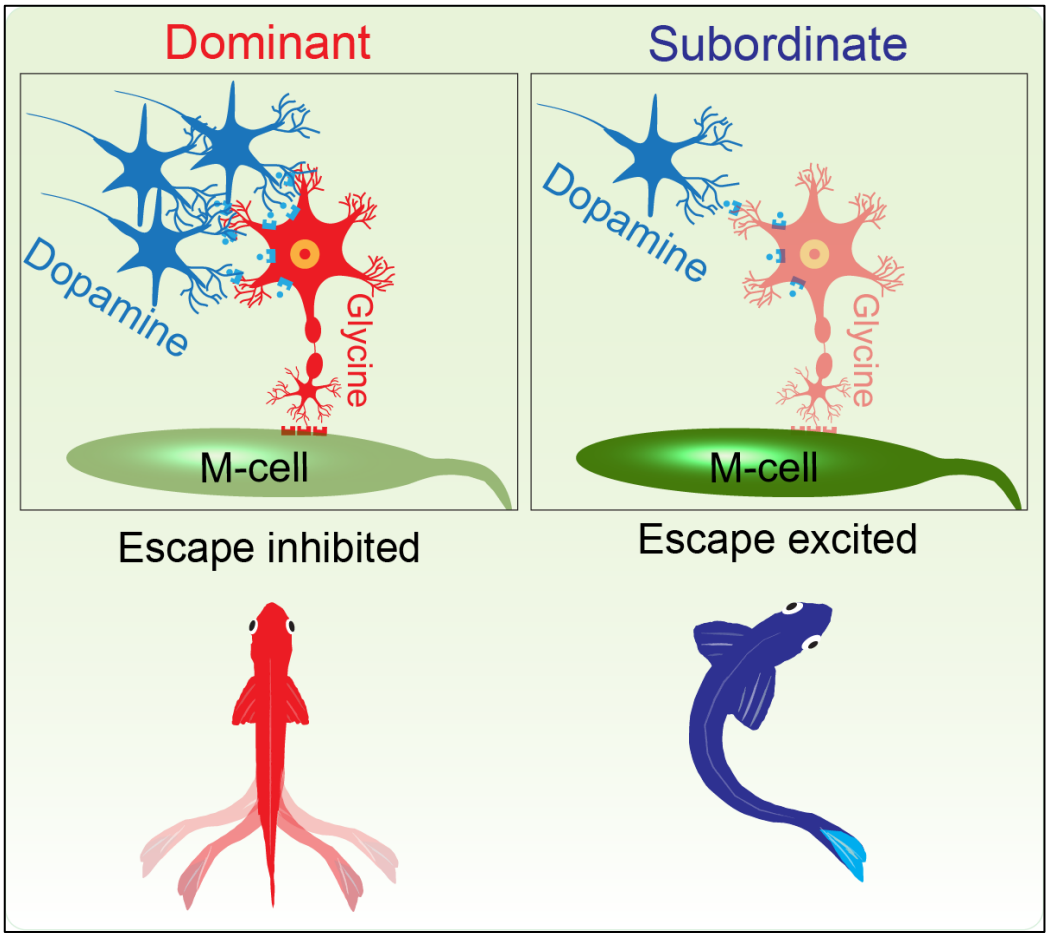

Figure 9. Neuromodulatory inputs on the M-cell. Schematic illustration suggesting DA indirectly modulating the M-cell by synapsing onto glycinergic neurons that are also modulating the M-cell.

glycinergic neurons to inhibit startle escape in dominants (Figure 9). In Subordinates, having fewer DA cells would reduce dopaminergic signaling, the consequences of which will lead to disinhibition of the M-cell (Figure 9). Although my results are consistent with this model, further studies examining synaptic transmission between dopaminergic and glycinergic neurons will be necessary to conclusively demonstrate that dopaminergic proliferation leads to enhanced synaptic contact with glycinergic neurons. Interestingly, morphological changes in hypothalamic DA cell number appear to be limited in scope because analysis of regional DA nuclei (PVOpa and PVOpb) showed no obvious morphological changes. This is consistent with their functional role in hormonal and homeostatic regulation. Collectively, the results show that the A11 is prone to social regulation by undergoing biochemical and morphological plasticity as animals adapt to new social conditions.

My results suggest morphological changes in that, the number of A11 DAT neurons expressing GFP are shifting as social relationships are maturing. Confirming whether the neurons in the transgenic zebrafish line, Tg(*dat:eGFP*), being counted are truly DAT expressing DA neurons or not is important. Previous studies have shown that the transgenic line Tg(*dat:eGFP*) zebrafish are expressing DAT in DA neurons (Xi et. al, 2011). Xi and colleagues after creating the transgenic line, double stained Tg(*dat:eGFP*) embryos with Mouse anti-GFP and Rabbit anti-TH to identify cells that are DA and expressing DAT. Although a successful transgenic line has been created to express *dat:eGFP* in Dopaminergic neurons, recent studies have shown that there are limitations to counting cells that express *dat:eGFP* as non-neuronal cells also express *dat:eGFP* (Asanuma et. al, 2014). Asanuma and colleagues stained healthy and hemi-parkinsonism rat brain sections with mouse anti-glial fibrillary acidic protein antibody, rabbit anti-L-DOPA polyclonal antibody, DA polyclonal antibody, and rabbit anti-DAT

polyclonal antibody. Results demonstrated that hemi-parkinsonism mice expressed higher levels of DAT in astrocytes compared to healthy rats (Asanuma et. al 2014). These results demonstrate that astrocytes also can express *dat*:eGFP. Future experiments for this specific project would need to be conducted to identify and confirm cells that not only express DAT, but that are dopaminergic neurons rather than astrocytes or any other type of neuron. To confirm whether the cells counted were truly DAT expressing DA neurons, I would perform an additional double stain with Anti-TH and Anti-GFP. Additionally, a MPTP (1-methyl-4-phenyl-1,2,3,6-tetrahydropyridine) stain, a neurotoxin, could be performed to examine DAT expressing cells undergoing cell death due to the toxin (Xi, et. al, 2011). MPTP is known to be metabolized into the toxic form MPP+ and brought into DA neurons by DAT (Wen et. al, 2008). After labeling for Anti-TH and Anti-GFP and then further staining for MPTP would show not only those cells that are DA, but those cells that undergo death are DA.

My results suggest that social dominance influences plasticity in the number of DAT expressing A11 neurons. These changes in the number of DAT expressing A11 neurons could be a result of DA phenotypic changes, neurogenesis, or neuronal loss. As a regulation of homeostasis, neurons can undergo phenotypic plasticity by changes in neurotransmitter phenotype (Demarque and Spitzer, 2012). Moreover, the number of neurons expressing dopamine can increase or decrease in response to spontaneous calcium spike changes (Demarque and Spitzer, 2012). Transcription factors involved in controlling the synthesis of different neurotransmitter molecules have been extensively studied (Cheng et. al, 2003). In dopamine, the nuclear transcription factor Nurr1 is involved in neuronal development and maintaining DA phenotype (Partington et. al, 2021). Partington and colleagues demonstrated changes in DA number across time with Nurr1-null heterozygous mice by measuring circadian fluctuations in

the number of DA neurons (Partington et. al 2021). Their results demonstrated that Nurr1 deficient mice models showed no differences in DA neurons over time (Partington et. al, 2021). Overall, DA could be phenotypically changing explaining differences in DAT expressing A11 Type I cell numbers.

The differences in DAT expressing A11 Type I cells could also be due to neurogenesis. The zebrafish brain has been shown to constantly regenerate DA neurons within the diencephalon compared to mammalian brain (Schmidt et. al, 2013; Caldwell et al, 2018; Lindsey et al, 2018). Multiple studies inducing lesions within the DA diencephalic region in amphibians and other vertebrate species have also demonstrated full capability of regeneration (Parish, et al. 2007). More interestingly, depending on the specific DA nuclei, regenerative capacity has been shown to vary (Caldwell et al, 2018). Whether the DAT expressing A11 Type I cells can fully recover from chronic, repeated social isolation or submission remains unknown. Neurogenesis is complex to capture as brains regions are rapidly producing proliferating cells, and not all fully reach maturity, making regional distribution of newly born neurons not uniform (Schmidt et. al, 2013; Zhao and Praag, 2020). Furthermore, genetics, environmental factors, and age influence the rate of neurogenesis. To study neurogenesis, finding markers to complete immunohistology of the DA cells is critical. It would be important to capture all stages of neurogenesis in a time course order to have a more accurate representation, and the utilization of BrdU (Bromodeoxyuridine) marker would be beneficial to capture adult neurogenesis (Zuo et al. 2019). BrdU is a synthetic thymidine nucleoside analog that substitutes thymidine during the S phase of the cell cycle and integrates into the newly synthesized DNA (Zuo et al. 2019). Once zebrafish brain tissue samples have been treated with BrdU and denatured to expose the antigen, an anti-BrdU antibody can be applied to distinguish A11 DAT type I cells that are BrdU positive and actively dividing (Grandel et al. 2006).

While neurogenesis could be occurring, cell death could be taking place as well. To examine if DAT expressing A11 Type I cells are undergoing cell death, using markers such as Caspase 3, a cysteine aspartic protease that cleaves cellular targets initiating apoptosis, or performing a TUNEL Assay can determine whether cell death is occurring. Then, comparison of DAT expressing A11 Type I cells that are expressing the specific cell death marker to total DAT expressing A11 Type I cells would be completed. When comparing the total number of cells undergoing neurogenesis and cell apoptosis in all social phenotypes, I would expect dominants to have more cells undergoing neurogenesis, and subordinates undergoing more cell death.

Coupled with changes in cell number, my results also show status-dependent synaptic plasticity in DAT expressing A11 Type I cells. Histological staining using PSD-95 antibody showed that subordinates had an increased number of DAT cells expressing PSD-95 compared to dominants and communals. Higher expression of PSD-95 in subordinates could be a result of increased pre-synaptic glutamatergic input onto the DAT expressing A11 cells. PSD-95 is known to be denser around excitatory synapses, receptors NMDA and AMPA, that are glutamatergic and has a potential role in regulating synaptic efficacy (Ehrlich and Malinow, 2004). In correlation with Drd1 receptor activation enhancing NMDA receptor activation, overexpression of Drd1 and NMDA receptors mediates neurotoxicity in the brain caused by trauma, stress, and even is associated with neurodegenerative diseases (Zhang et al. 2009). It is thought that PSD-95 facilitates Drd1 and NMDA interaction. Further experiments would need to be conducted to see the relationship of glutamatergic input to the DAT expressing A11 Type I cells by using a double labeled transgenic fish line, Tg(*vglut2 RFP;dat:eGFP*). This line not only expresses eGFP in all dopaminergic cells, but it also expresses RFP in all glutamatergic cells within the brain. By using this line, we could also count the number of glutamatergic cells within the A11 region and calculate

how close in proximity these cells are to the DAT expressing A11 Type I cells. I would predict that subordinates would have more glutamatergic neurons providing input onto the DAT cells, which would explain the higher expression of PSD-95 in the DAT expressing A11 cells.

A11 morphological plasticity is likely to impact A11 functional activity in how the A11 network integrates social cues and relays that information to spinal cord circuits. To investigate the consequences of social status dependent relationships on the functionality of the A11 cells, future experiments studying the dynamics changes of DA excitability could be studied. Utilizing calcium imaging or performing more immunohistological staining could answer this question. Two-photon calcium imaging has previously been done in larval zebrafish expressing channelrhodopsin-2 (ChR2) in th2+ neurons within the posterior hypothalamus (A9-A11 DA nuclei) (Barrios et al.,2020). In the larval zebrafish, th2+ neurons within the Posterior Tuberculum, intermediate hypothalamus, and caudal hypothalamus comprise of a periventricular network and have fast, phasic activity beginning within a few hundred milliseconds of onset locomotor behaviors (Barrios et al. 2020). Performing calcium imaging in dominants, subordinates, and communals could determine the changes in functional activity of the DAT expressing A11 type I cells as social status dependent relationships are maturing. In addition, markers for activation are readily available including c-Fos and rPS6. C-Fos is an immediate early gene that is induced by second messenger signals when there are changes in neuronal activity (Perrin-Terrin et al., 2016). Although, there are limitations to c-Fos detection as the protein has a half-life of 90-100 minutes. Its expression can be affected by unintended exposure to stress during experimental treatment, therefore would require immediate tissue extraction following any physiological stimulus (Herdegen and Leah 1998). C-Fos detection can be completed *ex vivo* and *in vivo.* Another marker that could be used to stain for activation is the

ribosomal protein S6 (rpS6). This protein is an important structural component localized between the large and small ribosomal unit. In previous studies, rpS6 has a profound role in translating a subset of mRNAs that alters synaptic plasticity and causes behavioral changes (Puighermanal et al., 2017). By staining DAT expressing A11 type 1 cells with either rPS6 or c-Fos, the effect of social status-dependent relationships on the functionality could provide new insights on how changes in morphological plasticity of the A11 translates into functional changes in A11 network activity.

Finally, my results show that the morphological differences in A11 cell number and synaptic density are socially induced and are not due to innate differences. When submissive fish were given the opportunity for social ascent, they quickly adapted their motor activity to reflect dominant status (Figure 8A, B). They reduced their startle sensitivity and increased their swimming activity. This correlated with significant proliferation in A11 cell number. However, behavioral adaptation and morphological plasticity in A1l during social descent were less obvious (Figure 8C). Dominant animals that lost their social status and became submissive (D→S) did not increase their startle sensitivity, nor did they decrease their swimming to subordinates levels as was predicted. However, those dominants that became submissive (D→S) showed a significant decline in A11 cell number. This suggests those former dominant animals were reluctant to give up their dominance status, and behavioral adaptations to new social conditions may not necessarily correlate completely in the short-term with A11 morphological plasticity. Secondly, the results suggest that brain nuclei involved in motivation and aggression may undergo physiological plasticity at different rates compared to the A11 nucleus. Perhaps it is likely that the differences in startle sensitivity and swimming frequency would become more pronounced with extended pairing beyond two weeks to ensure the full maturation of the new

social order. It is noteworthy to highlight that subordinates that remained submissive during the second pairing; thus, having been submissive for a total of 28 days, displayed depressive like behavior whereby their swimming activity declined even more than two weeks earlier. But most remarkably, their startle sensitivity began to shift in the opposite direction and became less sensitive to startle stimuli compared to short-term social submissives. This phenomenon of learned helplessness has been studied extensively and is described as the animals' failure to escape shock induced by uncontrollable aversive events. It was discovered half a century ago by Seligman and Maier who theorized that animals learned that outcomes were independent of their responses, that nothing they did really mattered, and that this learning undermined trying to escape (Seligman and Maier 1967; Maier and Seligman, 2016). Previous work in our lab showed exposing zebrafish to an extended duration of social stress (2 and 3 months) causes depressive like behavior in submissive fish, and they display characteristics of learned helpless in which depressed fish reduce their swimming activity more significantly compared to short-term submissives, and their startle escape response sensitivity declines dramatically (Sanders and Issa, unpublished observations). In this study, we have some evidence that support those results. Comparison of the startle escape response sensitivity in 14-days subordinates to those of 28-days long subordinates shows significant difference (Compare Figure 4C to Figure 7B). 28-days of social submission appears to cause those animals to reduce their startle sensitivity with a further decline, albeit modest, in swimming frequency compared to 14-days social submissives. Extended exposure to social stress beyond 28-days is likely to further amplify and fully manifest the effects of learned helplessness. The neurobiological bases of learned helpless has been examined, and it was noted serotonergic involvement in the induction of learned helplessness whereby reduced serotonergic neurons firing activity of the Dorsal Raphe nucleus and levels of

serotonin release causes rats to not escape (Hashimoto et al. 2021). We would need to further conduct those experiments and could extensively study levels of serotonin present in the Dorsal Raphe nucleus within each fish and compare those levels. Thus, it is predicted that depressed subordinates will show lower levels of serotonin in the Raphe nucleus. Further work is necessary to examine the relationship between serotonergic involvement in learned helplessness and likely A11 DA cellular loss.

In conclusion, this study demonstrates that social status affects motor activity and the morphological architecture of hypothalamic A11 DA nucleus involved in regulating the sensitivity of the startle escape M-cell circuit. Results show social status-dependent differences in cellular plasticity in dopaminergic cell number and synaptic density. Secondly, social reversal correlates, to an extent, with behavioral adaptations and plasticity in DAT expressing A11 Type I cell number. The results are consistent with our current model whereby increased dopaminergic synaptic drive onto hindbrain glycinergic neurons leads to functional adaption of the startle escape circuit. Collectively, this study highlights the impact of social factors in inducing morphological and functional plasticity, the basic mechanistic principals of which are likely present in other social species and can be studied in mammalian brain.

REFERENCES

Asanuma M, Miyazaki I, Murakami S, Diaz-Corrales FJ, & Ogawa N (2014) Striatal Astrocytes Act as a Reservoir for L-DOPA. *PLoS One* 9(9): e106362

Barrios JP, Wang Wei-Chun, England R, Reifenberg E, Douglass AD (2020) Hypothalamic Dopamine Neurons Control Sensorimotor Behavior by Modulating Brainstem Premotor Nuclei in Zebrafish. *Current Biology* 30(23): 4606-4618

Bátora D, Zsigmond A, Lőrincz IZ, Szegvári G, Varga M, Málnási-Csizmadia A (2021) Subcellular Dissection of a Simple Neural Circuit: Functional Domains of the Mauthner-Cell During Habituation. *Frontiers in Neural Circuits* 15:648487

Caldwell LJ, Davies NO, Cavone L, Mysiak KS, Semenova SA, Panula P, Armstrong AD, Becker CG, and Becker T (2019) Regeneration of Dopaminergic Neurons in Adult Zebrafish Depends on Immune System Activation and Differs for Distinct Populations. *Journal of Neuroscience* 39(24): 4694-4713

Chen L, Samad OA, Xu Y, Mizuguchi R, Luo P, Shirasawa S, Goulding M, & Ma Q (2005) LBX1 and Tlx3 are opposing switches in determining GABAergic versus glutamatergic transmitter phenotypes. *Nat Neurosci*. 8:1510-1515

Clemens S, Rye D, & Hochman, S. (2006). Restless legs syndrome: revisiting the dopamine hypothesis from the spinal cord perspective. *Neurology*, 67(1):125-130

Clements KN, Heagy FK, Blain E, Ward J, Issa FA (2020). Repeated Social Defeat Affects Dopaminergic Modulation of Spinal Motor Circuits. *Integr. and Comp. Biol.* 60, E41-E41

Clements KN, Miller, TH, Keever, J, Hall AM, Issa FA (2018). Social status related differences in motor activity between wild type and mutant zebrafish. *The Biological Bulletin* 235(2): 71-82.

Cunha-Bang Sofi da, et. al (2017) Violent offenders respond to provocations with high amygdala and striatal reactivity. *Social cognitive and Affective Neuroscience* (5)12: 802-810

Demarque M and Spitzer NC (2012) Neurotransmitter phenotype plasticity: an unexpected mechanism in the toolbox of network activity homeostasis. *Dev Neurobiol.* 72(1):22-32

Eaton RC, Bombardieri RA, Meyer DL (1977) The Mauthner-Initiated Startle Response in Teleost Fish. *J Exp Biol* 66(1): 65-81

Eaton RC, Lee RKK, & Foreman MB (2001) The Mauthner cell and other identified neurons of the brainstem escape network of fish. *Progress in Neurobiology* 63(4):467-485

Ehrlich I & Malinow R (2004) Postsynaptic density 95 controls AMPA receptor incorporation during long-term potentiation and experience-driven synaptic plasticity. *J Neurosci*. 24(4):916-927

Felicity A Huntingford (1987) Animal Conflict. Chapman and Hall, London. 22

Filby AL, Paull GC, FA Hickmore T, Tyler CR (2010) Unravelling the neurophysiological basis of aggression in a fish model. *BMC Genomics* 11,498

Grandel H, Kaslin J, Ganz J, Wenzel I, & Brand M (2006) Neural stem cells and neurogenesis in the adult zebrafish brain: Origin, proliferation dynamics, migration, and cell fate. *Developmental Biology* 295(1):263-277

Haehnel-Taguchi M, Fernandes AM, Bohler M, Schmitt I, Tittel L, Driever W (2018) Projections of the diencephalospinal dopaminergic system to peripheral sense organs in larval zebrafish (*Danio rerio*). *Front Neuroanat* 12:20

Han Y, Chen L, Liu J, Chen J, Wang C, Guo Y, Yu X, Zhang C, Chu H, & Ma H (2022) A Class I HDAC Inhibitor Rescues Synaptic Damage and Neuron Loss in APP-Transfected Cells and APP/PS1 Mice through the GRIP1/AMPA Pathway. *Molecules* 27(13):4160.

Hashimoto K, Yamawaki Y, Yamaoka K, Yoshida T, Okada K, Tan W, Yamasaki M, Matsumoto-Makidono Y, Kubo R, Nakayama H, Kataoka T, Kanematsu T, Watanabe M, Okamoto Y, Morinobu S, Aizawa H, Yamawaki S (2021) Spike firing attenuation of serotonin neurons in learned helplessness rats is reversed by ketamine, *Brain Communications*, 3(4)

Herdegen T, Leah JD (1998) Inducible and constitutive transcription factors in the mammalian nervous system: control of gene expression by Jun, Fos and Krox, and CREB/ATF proteins. *Brain Res Rev* 28(3):370–490

Humble F, Berk M (2003) Pharmacological management of aggression and violence. *Hum Psychopharmacol Clin Exp* 18(6): 423-436

Ikemoto S, Panksepp J (1999) The role of nucleus accumbens dopamine in motivated behavior: a unifying interpretation with special reference to reward-seeking. *Brain Res Rev* 31(1):6-41

Issa FA, Mazzochi C, Mock AF, Papazian DM (2011) Spinocerebellar Ataxia Type 13 Mutant Potassium Channel Alters Neuronal Excitability and Causes Locomotor Deficits in Zebrafish. *Journal of Neuroscience* 31(18):6831-6841

Koblinger, K., Füzesi, T., Ejdrygiewicz, J., Krajacic, A., Bains, J. S., & Whelan, P. J. (2014). Characterization of A11 neurons projecting to the spinal cord of mice. *PloS one 9*(10)

Langheinrich U (2003) Zebrafish: A new model on the pharmaceutical catwalk. *Bioessays* 25(9):904-912

Lorenz K (2005) On Aggression. *Routledge* pgs. 22-23

Lindsey BW, Douek AM, Loosli F, Kaslin J (2018) A Whole Brain Signaling, Embedding, and Clearing Pipeline for Adult Zebrafish to Visualize Cell Proliferation and Morphology in 3-Dimensions. *Front. Neurosci.* 11:750

Maier, SF, & Seligman, ME (2016). Learned helplessness at fifty: Insights from neuroscience. *Psychological review* 123(4):349–367

Meiser J, Weindl D, Hiller K (2013) Complexity of Dopamine Metabolism. *Cell Communication and Signaling* 11:34

Miller TH, Clements K, Ahn S, Park C, Issa, FA (2017) Social Status-Dependent shift in neural circuit activation affects decision making. *Journal of Neuroscience* 37(8) 2137-2148.

Mu Y, Li X, Zhang B, Du J (2012) Visual inputs modulates audiomotor function via hypothalamic dopaminergic neurons through a cooperative mechanism. *J.Neuron* 75(4):688-99
Nakajo H et al. (2020) Hunger Potentiates the Habenular Winner Pathway for Social Conflict by Orexin-Promoted Biased Alternative Splicing of the AMPA Receptor Gene. *Cell Reports* 12:31

Norton W, Bally-Cuif L (2010) Adult zebrafish as a model organism for behavioral genetics. *BMC Neurosci* 11:90

O'Connell LA, Hofmann HA (2012). Evolution of a vertebrate social decision-making network. *Science* 336(6085)

O'Connell LA, Hofmann HA (2012) Social status predicts how sex steroid receptors regulate complex behavior across levels of biological organization. *Endocrinology* 153(3):1341-51

Oliveira RF, Silva JF, Simões JM (2011) Fighting Zebrafish: Characterization of Aggressive Behavior and Winner-Loser Effects. *Zebrafish* 8(2):73-81

Parish,CL, Beljajeva A, Arenas E, & Simon A (2007). Midbrain dopaminergic neurogenesis and behavioural recovery in a salamander lesion-induced regeneration model. *Development* (Cambridge, England) 134(15), 2881–2887.

Partington HS, Nutter JM, & Eells JB (2021) Nurr1 deficiency shortens free running period, enhances photoentrainment to phase advance, and disrupts circadian cycling of the dopamine neuron phenotype. *Behav Brain Res.* 411:113347

Perrin-Terrin AS, Jeton F, Pichon A, Frugière A, Richalet JP, Bodineau L, Voituron N (2016) The c-FOS Protein Immunohistological Detection: A Useful Tool As a Marker of Central Pathways Involved in Specific Physiological Responses In Vivo and Ex Vivo. *J Vis Exp* 110:53613.

Pereda AE, Nairn AC, Wolszon LR, Faber DS (1994) Postsynaptic modulation of synaptic efficacy at mixed synapses on the Mauthner cell. *Journal of Neuroscience* 14(6):3704-3712

Puighermanal E, Biever A, Pascoli V, Melser S, Pratlong M, Cutando L, Rialle S, Severac D, Boubaker-Vitre J, Meyuhas O, Marsciano G, Lüscher C and Valient E (2017) Ribosomal Protein S6 Phosphorylation Is Involved in Novelty-Induced Locomotion, Synaptic Plasticity, and mRNA Translation. *Front. Mol. Neurosci* 10:419

Ryczko D, Grätsch S, Auclair F, Dube C, Bergeron S, Alpert MH, Cone JJ, Roitman MF, Alford S, & Dubuc R (2013) Forebrain dopamine neurons project down to a brainstem region controlling locomotion. PNAS 110(34)

Schmidt R, Strahle U, & Scholpp S (2013) Neurogenesis in zebrafish- from embryo to adult. *Neural Development* 8(3)

Schwab-Reese LM, Parker EA, and Peek-Asa C. (2020) The interaction of Dopamine genes and Financial stressors to Predict Adulthood Intimate Partner Violence Perpetration. *Journal of Interpersonal Violence*. 35(5-6):1251-1268

Seligman MEP, Maier SF. (1967). Failure to escape traumatic shock. Journal of Experimental Psychology. 74:1–9

Smeets WJ, González A (2000) Catecholamine systems in the brain of vertebrates: new perspectives through a comparative approach. *Brain Res Rev* 33(2-3):308-379

Takahashi A, Flanigan ME, McEwen BS, Russo SJ (2018) Aggression Spcial Stress, and the Immune system in Humans and Animal Models. *Front. Behav. Neurosci*. 12:56

Tay TL, Ronneberger O, Ryu S, Nitscheke R, Driever W (2011) Comprehensive catecholaminergic projectome analysis reveals single-neuron integration of zebrafish ascending and descending dopaminergic systems. *Nat Commun* 2:171

Thomas JH. Chen, Kenneth Blum, Daniel Mathews, Larry Fisher, Nancy Schnautz, Eric R. Braverman, John Schoolfield, Bernard W. Downs, David E. Comings (2005) Are dopaminergic genes involved in a predisposition to pathological aggression?: Hypothesizing the importance of "super normal controls" in psychiatricgenetic research of complex behavioral disorders. *Medical Hypotheses* 65(4):703-707

Veldman M, Lin S (2008) Zebrafish as a Developmental Model Organism for Pediatric Research. *Pediatr Res* 64:470-476.

Watanabe N & Yamamoto M (2015) Neural mechanisms of social dominance. *Front. Neurosci*. 9:15

Weitekamp CA, Nguyen J, Hofmann HA (2017) Social context affects behavior, preoptic area gene expression, and response to D2 receptor manipulation during territorial defense in a cichlid fish. *Genes Brain Behav*.16(6):601-611

Wen L, Wei W, Gu W, Huang P, Ren X, Zhang Z, Zhu Z, Lin S, & Zhang B (2008) Visualization of monoaminergic neurons and neurotoxicity of MPTP in live transgenic fish. *Dev Biol* 314:84-92

Xi Y, Yu M, Godoy R, Hatch G, Poitras L, & Ekker M (2011) Transgenic Zebrafish Expressing Green Fluorescent Protein in Dopaminergic Neurons of the Ventral Diencephalon. *Developmental Dynamics,* 240:2539-2547

Zhang J, Xu T, Hallet P, Watanabe M, Grant S G.N., Isacson O, & W Yao (2009) PSD-95 Uncouples Dopamine-Glutamate Interaction in the D1/PSD-95 /NMDA Receptor Complex. *J Neurosci.* 29(9): 2948-2960

Zhao X & Praag H (2020) Steps towards standardized quantification of adult neurogenesis. Nature Communications 11, 4275

Zuo Y, Wang J, Enkhjargal B, Doycheva D, Yan X, Zhang JH, & Liu F (2019) Neurogenesis changes and the fate of progenitor cells after subarachnoid hemorrahage in rats. Experiment Neurology 311: 274-284

\

APPENDIX

Animal Care and Use Committee
003 Ed Warren Life Sciences Building | East Carolina University | Greenville NC 27834 – 4354
252-744-2436 office | 252-744-2355 fax

May 6, 2022

Fadi Issa, Ph.D.
Department of Biology, ECU

Subject: Protocol D320b, original approval date 11/06/2020

Dear Dr. Issa:

The amendment#2 to your Animal Use Protocol entitled, “Social Status-dependent regulation of an identified brain circuit” (AUP#D320b) was reviewed by this institution's Animal Care and Use Committee on 05/06/2022. The following action was taken by the Committee:

"Approved as submitted"

Please contact Aaron Hinkle prior to any hazard use

A copy of the protocols is enclosed for your laboratory files. Please be reminded that all animal procedures must be conducted as described in the approved Animal Use Protocol. Modifications of these procedures cannot be performed without prior approval of the ACUC. The Animal Welfare Act and Public Health Service Guidelines require the ACUC to suspend activities not in accordance with approved procedures and report such activities to the responsible University Official (Vice Chancellor for Health Sciences or Vice Chancellor for Academic Affairs) and appropriate federal Agencies. Please ensure that all personnel associated with this protocol have access to this approved copy of the AUP/Amendment and are familiar with its contents.

Sincerely yours,

Susan McRae, Ph.D.
Chair, Animal Care and Use Committee

JD/GD

enclosure